Development of an electrochemical biosensor for detection of cytokines simultaneously to cell stimulation

Ana Catarina de Almeida Barata, Instituto Superior Técnico, Portugal
catarina.barata@tecnico.ulisboa.pt

ABSTRACT

Microglia, the immune cells of the central nervous system (CNS), play an important role in both the normal function and the diseased behaviour of the CNS. Cytokine secretion is one of the most important categories of microglial function, modulating other cells' behaviour and being characteristic of pro- and anti-inflammatory responses to diverse stimuli. As such, microglia and cytokines are key players in determining progression or regression of pathology in the CNS and therefore cytokines can be used as biomarkers for diagnosing CNS disease. New methods for detecting and quantifying cytokines of interest are essential for studying their roles in both the healthy and diseased CNS. In this thesis an electrochemical biosensor based on electrochemical impedance spectroscopy (EIS) was developed, for pro-inflammatory cytokine tumour necrosis factor alpha (TNFα), with the functionalization of gold electrodes with anti-TNFα antibodies. The functionalization protocol was optimized to yield the most precise and accurate results possible with the shortest assay time, including a sample incubation time of 90 minutes with a sample volume of 1 μL. A calibration curve was obtained for this cytokine on a range of concentrations from 2.5 to 25 pg mL^{-1}, with a Limit of Detection (LOD) of 2.67 pg mL^{-1}. The biosensor shows selectivity against cytokines interleukin 4 (IL-4) and interferon gamma (IFN-γ), and a small interference with IL-10. Nevertheless, the results obtained, when testing cocktails including all four cytokines in a 0.9% NaCl solution, were quite accurate in terms of TNFα concentration. Overall, this biosensor shows several advantages over standard method ELISA, being capable of detecting TNFα at lower concentrations, with less sample volume and incubation time, revealing itself quite promising in this early stage of development. With further optimization work on functionalization and calibration, this biosensor could be the starting point for a useful detection and quantification device both in academic research and clinical diagnosis.

Keywords: microglia, cytokine, TNFα, electrochemical impedance spectroscopy, biosensor

1 INTRODUCTION

The central nervous system (CNS) consists of neurons, and glia cells (oligodendrocytes, astrocytes and microglia (MG) cells). Glial cells are involved in several aspects of brain function, including: insulation and support of neurons, synapse formation and transmission regulation, and maintenance and protection of the CNS.[1,2] In the mature brain, infiltration of immune cells, such as monocytes and macrophages is almost negligible and therefore MG, the immune cells of the CNS, constitute an autonomous and self-renewed population in this system.[3]

MG functions in the CNS can be as diverse as positioning neurons and organizing axon projections[4], as well as promoting neuronal differentiation[5] and survival[6] in the developing brain; and expressing phagocytic housekeeping behaviour, collecting apoptotic or damaged cells, foreign material and DNA fragments[7], for example removing the large number of cells in the neocortex that die in the course of normal remodelling of the fetal brain[8]. When exposed to infectious organisms, bacteria and virus, MG can eliminate them through phagocytosis and function as antigen-presenting cells, recruiting T-cells and directing them to a specific response best-suited for the elimination of specific pathogens.[9,10] Cytokine secretion is, alongside secretion of other proteins and chemical species, the key player driving most of the MG functions mentioned above. In this manner, MG can modulate other brain cells, as well as activate T-cells, thus deciding the outcome of the brain disturbance, which can have detrimental or beneficial consequences.[2,11,12]

Multiple MG activation states can be found, and MG is able to switch from 'resting' default, moving and interacting with the surrounding environment, into an activated M1-like or M2-like state.

M1 is induced by T helper 1 (Th1) cytokines, interferon gamma (IFN gamma), tumour necrosis factor alpha (TNFα), and lipopolysaccharide (LPS). The M1 state is associated with the production of pro-inflammatory cytokines (Interleukins and TNFα), cytotoxic substances (oxygen-free radicals and NO), increased phagocytic activity and tumour resistance.[13,14] The M2 is induced by Th2 cytokines interleukin 4 and 10 (IL-4 and IL-10), that triggers anti-inflammatory responses (IL-10, transforming growth factor beta (TGF-β)), and promotes tissue repair (extracellular matrix components (ECM), arginase1).[13,14]

Importantly, the outcome of the inflammatory response depends on the tight balance of M1 and M2 cell numbers, even though a specific cytokine-activated MG cell's neuroprotective/pro-neurogenic or neurodegenerative/anti-neurogenic behaviour is context-dependent. Persistent cytokine production from M1-like chronic activated MG results in chronic neuroinflammation and is associated with cell loss, tissue damage as well as with the development of neurodegenerative diseases[15]. Whereas an M2 phenotype may promote cell protection, regeneration, plasticity, being associated with neuroprotection[16]. However, the precise balance between MG cell types during disease conditions and how it impacts pathogenesis remains unknown. A MG misresponse, either pro- or anti-inflammatory, can be observed in several diseases including Alzheimer's disease[17], Parkinson's disease[18] and Multiple Sclerosis[19].

Pro-inflammatory cytokines secreted by activated M1 MG are TNFα, IL-1, IL-6 IL-12, IL-16 and IL-23.[11]. These have negative effects on the developing and adult CNS and can be induced *in vitro* by exposure to certain molecules, of which LPS is the most commonly used, or other cytokines like IFN-γ.[20]

Anti-inflammatory cytokines produced by MG, IL-10, TGF-β and IL-4, have immunosuppressive effects and promote neuronal differentiation and growth. These can be induced *in vitro* by Prostaglandin E2 (PGE2) [21] for example, while IL-10 promotes IL-4 activity[22].

Due to the localized effect on the CNS parenchyma and the presence of the blood brain barrier (BBB), blood samples aren't an optimal option for analysing the presence of MG secreted cytokines.[23] Lacrimal fluid[24] would be an interesting alternative to blood and cerebrospinal fluid, whose collection is highly invasive, despite providing small sample volumes.

Assessing cytokine profiles in small sample volumes, represents a significant technical challenge, particularly when cytokines are present at low concentrations. In order to detect and quantify cytokine levels, a plethora of protocols can be used. These methods range from the historically gold standard method, sandwich enzyme-linked immunosorbent assay (ELISA); to the new forefront method, bead based multiplex immunoassays (MIA), which permits detection of several cytokine at once. ELISA is the most commonly used and while it has good detection limits (4 pg mL^{-1} for TNFα for example[25]), the overnight incubation for samples as well as the required sample volume of 100 μL are parameters that can be improved upon by a new detection and quantification method.

The proposed method is a biosensor with an electrochemical platform functionalized with specific antibodies for TNFα, whose concentration will be determined through electrochemical impedance (EIS) measurements.

Considering an electrode with a diameter of a millimetre, when compared to the volume of an ELISA well, much less sample is needed, with sample volumes below the μL being sufficient. The electrical nature of the measurements will possibly make for a lower detection limit of cytokine concentration than the one permitted with ELISA, as well as allow for higher sensitivity.

The goal of this project is the development this biosensor, that can accurately and specifically detect and quantify TNFα. The study will focus on the functionalization of electrodes with a cross-linker, anti-TNFα antibodies and blocking agent to obtain a biosensor calibrated to accurately measure the concentration of this cytokine in a sample. The biosensor will be tested for accuracy, specificity and cross-reactivity while testing cytokine samples in different media. Finally, a cross-validation of sample testing results will be done with ELISA as a reference method.

2 MATERIALS AND METHODS

2.1 Setup

DropSens C223AT chips (Figure 1) with screen-printed gold electrodes (working electrode diameter: 1.6 mm) were used for developing the biosensors. During incubations, the chips were kept in a humid chamber, covered with aluminium foil to maintain darkness. The EIS measurements were performed by a potentiostat (Metrohm Autolab PGSTAT302N with a frequency analyser module FRA32M) to which the chips were linked with a connector (DropSens DSC). NOVA software (version 2.0.2, Metrohm Autolab) was used to manipulate the potentiostat and process data. The R_{et} values were obtained from a fit and simulation module on the NOVA software to adapt the data to the equivalent circuit [R(Q[RW])].

Figure 1: DropSens gold printed electrodes chip covered in redox probes solution and inserted into the connector.

2.2 Reagents and buffers preparation

Phosphate buffer (PB), pH 7.4, was prepared by mixing solutions of 0.100 M NaH_2PO_4 and 0.100 M of Na_2HPO_4. For these, NaH_2PO_4 powder (Sigma) was dissolved into Milli-Q water and the same procedure was repeated for Na_2HPO_4 (Sigma). The 0.1 M PB solution was kept at 4º C and was filtered before each assay. Phosphate buffered saline (PBS) was prepared by dissolving one compressed tablet (Sigma) in 200 mL of Milli-Q water to obtain a solution with pH 7.4 and 10 mM phosphate buffer, 2.7 mM potassium chloride and 137 mM sodium chloride. A stock solution of 10 mM of PBS was kept at 4º C.

For one of the tests in sensor validation, cytokines were diluted in cell culture medium. This was Dulbecco's modified Eagle's medium (DMEM, Gibco, ref. 31966021, with high glucose, GlutaMAX^{TM} supplement and pyruvate) with 10% Fetal Bovine Serum (FBS, Gibco). In the other validation test, the cytokines were diluted in a 0.9% NaCl (Sigma) solution in deionized water (DI water).

The electrolyte solution used for EIS measurements was a 10 mM PBS, 5 mM $[Fe(CN)_6]^{3-/4-}$ (prepared from 1 M $C_6FeK_3N_6$ (Sigma) and 1 M $C_6FeK_4N_6$ (Sigma) solutions in Milli-Q water) solution. These solutions were made fresh for use in each assay and the final probe solution was stored overnight when applicable at 4º C. During the assay, the probe solution was kept at room temperature in a flask covered with aluminium foil to protect it from the light.

The cross-linker used was Sulfosuccinimidyl 6-[3'(2-pyridyldithio)-propionamido] hexanoate (Sulfo-LC-SPDP, ThermoScientific) which was reconstituted by dissolving the powder in PB. Glycerol (Sigma) was added for a final solution of 10 mg mL^{-1} Sulfo-LC-SPDP, 5% glycerol. The solution was aliquoted in 10 µL volumes and stored at -20º C.

Human anti-TNFα antibody (Affymetrix, capture antibody from the ELISA Ready-SET-Go! Human TNFα kit[25]) was diluted in PB for a final concentration of 0.25 mg mL^{-1} and aliquoted in 10 µL volumes, which were stored at 4º C. Bovine Serum Albumin (BSA, Sigma) 1% solution in PB, was made fresh for each assay, and stored overnight when applicable at 4º C.

Human recombinant cytokines TNFα, IL-10, IL-4 and IFN-γ (all Affymetrix) were reconstituted in sterile DI water, from the lyophilized form according to the Certificate of Analysis provided by the brand. These solutions were aliquoted in 20 µL and stored at -80º C.

2.3 Electrochemical impedance spectroscopy measurements

EIS measurements were performed after each step of the protocol, including a bare reading at the beginning of the run. The chips were covered in the ferri-/ferrocyanide solution and EIS measurements were performed under a bias potential of 0.125 V, with a frequency range of 0.1-100000 Hz and an alternating current amplitude of 5 mV. The redox probes solution was then rinsed off with Milli-Q water and the chips dried under an N_2 stream.

2.4 Functionalization of electrodes

2.4.1 Covalent cross-linker immobilization

The electrodes were first cleaned with isopropanol (IPA) and Milli-Q water and dried with N_2. The working electrode was covered with 10 mg mL^{-1} of Sulfo-LC-SPDP, for 20 minutes, at room temperature, in dark humid atmosphere. The excess solution was rinsed with PB.

2.4.2 Antibody immobilization

The electrodes were functionalized with 0.25 mg mL^{-1} of anti-TNFα, for 2 hours, at room temperature and in humid atmosphere. The unbound antibody was rinsed off with PB.

2.4.3 Blocking of non-specific binding sites

After functionalization, the available surface of the working electrode was blocked using 1% BSA, for 1 hour, at room temperature and in humid atmosphere, after which the excess solution was rinsed off with PB.

2.5 Electrode calibration

Solutions of TNFα cytokine were sequentially incubated on the working electrode, for 90 minutes each, in humid atmosphere and at room temperature. The concentrations used, in multiple combinations, were 1, 2.5, 5, 10, 25, 50, 100, 150, 200 and 250 pg mL^{-1} of TNFα.

2.6 Specificity analysis

Negative controls for biosensor selectivity were performed with IL-10, IL-4 and IFN-γ cytokine solutions. Consecutive incubations of 10, 25, 50 and 100 pg mL^{-1} solutions of each cytokine were made for 90 minutes each, at room temperature and in humid atmosphere.

2.7 Cross-reactivity tests

Cytokine cocktails were made with cytokines diluted in either DMEM-10%FBS or 0.9% NaCl solution. The cocktails were incubated for 90 minutes in humid atmosphere and at room temperature. The different combinations of the four cytokines are detailed in Table 1.

2.8 Cross-validation with the reference method (ELISA)

Cross-validation of results was made with ELISA as a reference method, with material and reagents from the Affymetrix Human TNFα ELISA Ready-SET-Go! Kits, using the experimental procedure protocol provided in the kit.[25] The samples used were the same 0.9% NaCl diluted cytokine cocktails described in Table 1.

2.9 Electrochemical INL fabricated sensors

Initial tests were performed in parallel on chips containing electrodes with a thin gold surface of 100 nm, fabricated at INL. The chips and their structure can be seen in Figure 2. A connector developed at INL connected the chips to the potentiostat.

The INL electrodes have a smoother surface than the DropSens ones, but the work on these chips had to be discontinued due to external problems in the microfabrication process.

3 Results and Discussion

3.1 Functionalization protocol optimization

Most of the functionalization protocol was optimized, especially the duration of the incubations. The most relevant changes were achieved on the incubation times of the cross-linker and the cytokine.

3.1.1 Effect of incubation time, concentration and freshness of solution on Sulfo-LC-SPDP immobilization

Different incubation times of 20, 40 and 60 minutes, the effect of the age of the solution (aliquoted versus fresh) and the concentration, 1 and 10 mg mL^{-1}, were tested for Sulfo-LC-SPDP.

(a)

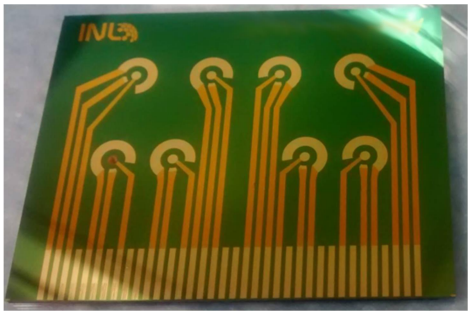

(b)

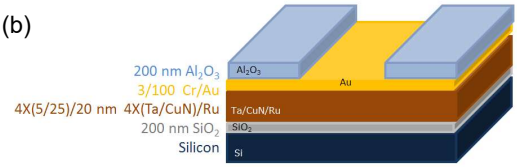

Figure 2: INL microfabricated chips with eight gold electrodes, on a silicon substrate: a photo of the chip (a) and the structure materials (b).

The results are shown in Figure 3, where $R_{et,1}$ is the R_{et} after Sulfo-LC-SPDP immobilization and $R_{et,0}$ is the bare measurement.

The incubation with the aliquoted solution of 10 mg mL^{-1} had a significant increase in R_{et} with incubation time, contrasting with the other solutions which showed a general stagnation after 40 minutes of incubation. A comparison was made on Sulfo-LC-SPDP and subsequent antibody immobilization using the aliquoted solution and the fresh solution, both with a concentration of 10 mg mL^{-1} and with an incubation period of 20 minutes. The results, illustrated in Figure 4, show the normalized R_{et} with Sulfo-LC-SPDP immobilization in (a), where $R_{et,1}$ is the R_{et} of Sulfo-LC-SPDP immobilization and $R_{et,0}$ is the bare measurement; and the normalized R_{et} with antibody incubation in (b), where $R_{et,1}$ is the R_{et} after antibody immobilization and $R_{et,0}$ is the R_{et} after Sulfo-LC-SPDP.

Table 1: Composition of the cytokine cocktail samples used in cross-reactivity and interference tests for the biosensor and in cross-validation with ELISA (only the 0.9% NaCl cocktails).

Medium	Cytokine cocktail samples
DMEM-10%FBS	Blank
	100 pg mL^{-1} TNFα
	100 pg mL^{-1} TNFα + 100 pg mL^{-1} IFN-γ
	100 pg mL^{-1} TNFα + 100 pg mL^{-1} IFN-γ + 100 pg mL^{-1} IL-10
	1000 pg mL^{-1} TNFα
	1000 pg mL^{-1} TNFα (diluted x10)
0.9% NaCl	Blank
	25 pg mL^{-1} TNFα
	25 pg mL^{-1} TNFα + 25 pg mL^{-1} IFN-γ + 25 pg mL^{-1} IL-4
	25 pg mL^{-1} TNFα +25 pg mL^{-1} IFN-γ + 25 pg mL^{-1} IL-4 + 25 pg mL^{-1} IL-10

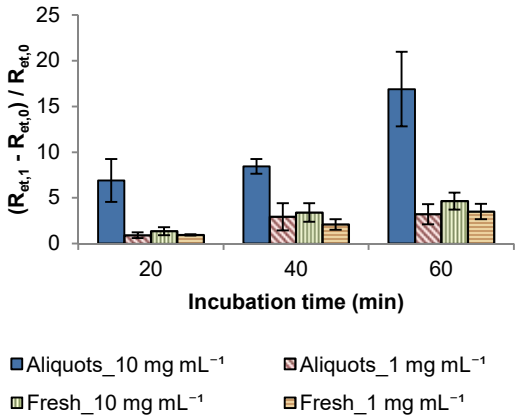

Figure 3: Comparison of normalized R_{et} measured after Sulfo-LC-SPDP over the incubation times, at different concentrations (1 and 10 mg mL^{-1} solution), and for fresh or aliquoted samples. Error bars represent the standard deviation.

Considering the increase of R_{et} after Sulfo-LC-SPDP immobilization over the bare reading was notably higher for the aliquoted solution than for the fresh one (Figure 4a), and the response after antibody immobilization was similar for both (Figure 4b), it can be proposed that the same percentage of immobilized cross-linker had antibody bound to it in both cases, and after 20 minutes the monolayer of Sulfo-LC-SPDP is totally assembled using the aliquoted 10 mg mL^{-1} solution. It was decided to continue to use the aliquoted solution of 10 mg mL^{-1} with an incubation time of 20 minutes. The reduced incubation time had the practical

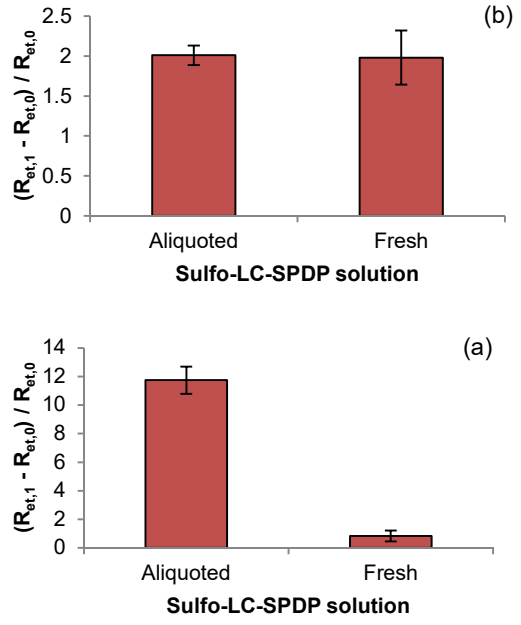

Figure 4: Comparison for aliquoted and fresh Sulfo-LC-SPDP solutions of normalized R_{et}: (a) R_{et} after Sulfo-LC-SPDP immobilization and (b) R_{et} after antibody immobilization. Error bars represent the standard deviation.

advantage of avoiding the drying of the Sulfo-LC-SPDP solution drop during the immobilization and speed-up the functionalization period.

3.1.2 TNFα binding time optimization

Incubation times of 20, 40, 60 and 90 minutes were tested, and the results are shown in Figure 5. A slight tendency can be observed where 90 minutes of incubation yield higher increases in R_{et} than those from 60 minutes of incubation. For this reason, the selected incubation time for TNFα was 90 minutes.

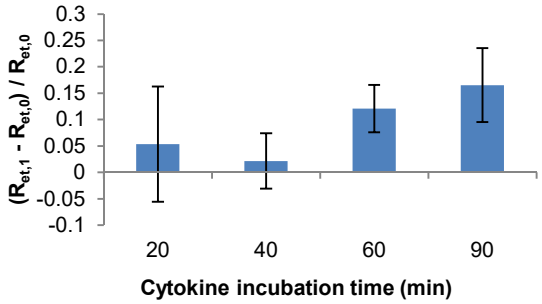

Figure 5: Comparison of normalized Ret after TNFα incubation for different incubation times. The error bars represent the standard deviation.

A longer incubation period was not tested during this project. The difference between the increases in R_{et} for 60 and 90 minutes was not very severe and it is admissible to believe that 120 minutes of incubation would not result in a much different response.

3.2 Calibration and sensor sensitivity

The first concentration range used for biosensor calibration was [25; 50; 100; 150; 200; 250] pg mL^{-1} of TNFα, which resulted in a plateau being reached after 50 pg mL^{-1}, suggesting electrode saturation. A lower range including the lower concentrations levels of the high range curve and two levels below the limit of detection (LOD) for ELISA (4 pg mL^{-1})[25] was then tested: [1; 2.5; 5; 10; 25; 50] pg mL^{-1}. This resulted in negative normalized R_{et} for the first two concentration levels suggesting that the LOD for this biosensor was at or above 2.5 pg mL^{-1}.

A third concentration range of [2.5; 5; 10; 25; 50; 100] pg mL^{-1} of TNFα was used for estimating another calibration curve, which is shown in Figure 6, where $R_{et,1}$ is the R_{et} measured after each cytokine incubation and $R_{et,0}$ is the value after blocking. The linear regression, which includes the concentration points from 2.5 to 25 pg mL^{-1} is given by Equation 1 and has an r-squared value of 0.9497.

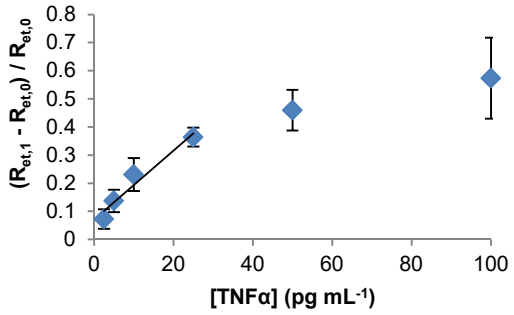

Figure 6: Variation of normalized Ret with TNFα concentration, for the final range of concentrations: [2.5; 5; 10; 25; 50; 100] pg mL^{-1}, with associated standard deviations. Linear regression representing the calibration curve over the lower range of the concentration levels.

$$\Delta \mathrm{R_{et}} TNF\alpha = \\ = (1.2 \pm 0.4) \times 10^{-2} \times [\mathrm{TNF\alpha}](\mathrm{pg\ mL^{-1}}) + \\ + (7 \pm 0.003) \times 10^{-2} \quad (1)$$

For this calibration curve, the limit of detection is 2.67 pg mL^{-1}, which confirms the interpretation that the 1 and 2.5 pg mL^{-1} concentration levels were below or at the LOD. This is a lower value than the theoretic LOD for ELISA (4 pg mL^{-1})[25], which confirms that this biosensor, can detect lower concentrations of TNFα than ELISA. In Figure 7, all three calibration curves are gathered, with $R_{et,1}$ as the R_{et} measured after each cytokine incubation and $R_{et,0}$ as the value after blocking. The linearity stages are common to all ranges, with a steep ascent until 50 pg mL^{-1} and a plateau starting after 50 pg mL^{-1}. On the other hand, when comparing all three calibration curves, it is possible to observe a cumulative effect due to the successive additions of TNFα (ascendant calibration) which affects the values of the rest of the concentrations. This is especially noticeable (Figure 7b) for the 25 and 50 pg mL^{-1} concentration levels, which are present in all the ranges. A calibration method that would avoid this issue would be to use each electrode to incubate and measure one single concentration level. This would result in more accurate calibrations with no accumulation effect and independent measurements for each point.

3.3 Specificity of the biosensor

In Figure 8 are the resulting plots of normalized R_{et} after each consecutive cytokine incubation, versus cytokine concentration, for IL-4, IFN-γ and IL-10, respectively. The range of concentrations tested was 10, 25, 50 and 100 pg mL^{-1} for each cytokine, encompassing the higher section of the calibration curve and higher concentrations to guarantee detection by the biosensor. In these figures, $R_{et,1}$ is the R_{et} measured after each cytokine incubation and $R_{et,0}$ is the value after blocking.

As observable in Figure 8a and 8b, the normalized R_{et} for both IL-4 and IFN-γ doesn't increase with successive incubations of higher concentrations. This means that the sensor does not detect any of the cytokines, being selective against both. For IL-10 (Figure 8c), it is possible to see some interference, implying that IL-10 is binding to the antibodies or to some other element in the biosensor non-specifically. This cross-reactivity isn't very significant when compared with the signal produced by TNFα, as can be seen in Figure 9, where $R_{et,1}$ is the R_{et} measured after each cytokine incubation and $R_{et,0}$ is the value after blocking.

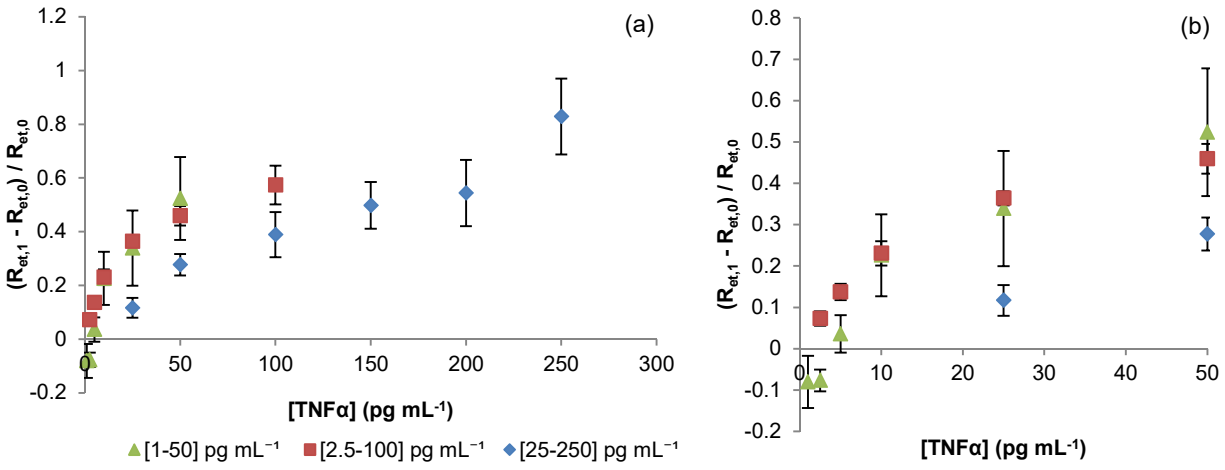

Figure 7: Juxtaposition of the curves of normalized Ret against concentration of TNFα, with the respective standard deviation for each point, for the three concentration ranges: [1-50] pg mL^{-1} (green triangles), [2.5-100] pg mL^{-1} (red squares) and [25-250] pg mL^{-1} (blue diamonds). (a) all concentrations tested, (b) inset of concentrations 1 to 50 pg mL^{-1}.

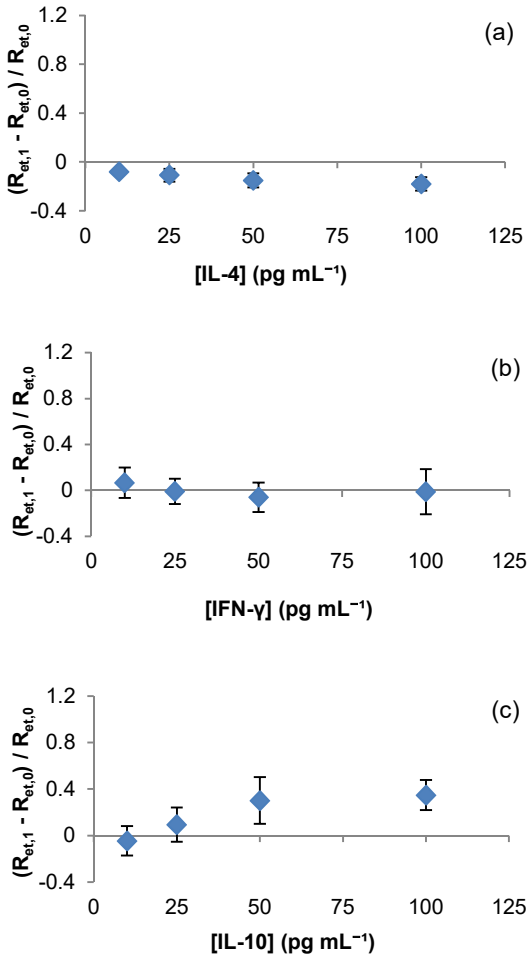

Figure 8: Variation of normalized Ret with cytokine concentration, with associated standard deviations, for each of the control cytokines: (a) IL-4, (b) IFN-γ and (c) IL-10.

3.4 Cross-reactivity tests

The results of the cross-reactivity tests on DMEM-10%FBS cocktails are illustrated in Figure 10. In this chart, $R_{et,1}$ is the R_{et} measured after the cocktail incubation and $R_{et,0}$ is the value after blocking. The measurements suffered from significant interferences. This is likely due to the medium itself and its complex matrix full of proteins and other compounds, as the interference exhibited by the solution diluted 10 times from the 1000 pg mL⁻¹ TNFα concentration is lower than all the others.

The 0.9% NaCl cytokine cocktails (Figure 11, where $R_{et,1}$ is the R_{et} measured after the cocktail incubation and $R_{et,0}$ is the value after blocking), however, presented less interference, with the blank itself showing decreases from the base but the cocktails having R_{et} increases that can be used with the calibration curve to calculate the concentration of TNFα. Subtracting the normalized R_{et} for the blank to each of the cocktails' normalized R_{et}, and

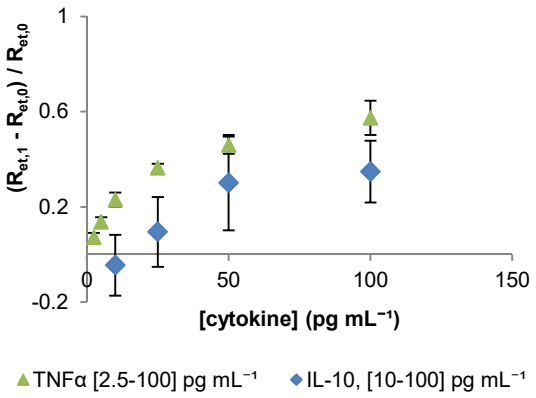

Figure 9: Comparison of normalized Ret for the negative control IL-10 cytokine in the tested [10-100] pg mL⁻¹ range (blue diamonds) with the final TNFα calibration curve on the range [2.5-100] pg mL⁻¹ (green triangles). Included are also the standard deviations for each point.

using the calibration curve obtained for the biosensor in Equation 1, the TNFα concentrations were interpolated for each of the 0.9% NaCl cocktails and are shown in Table 2, along with the standard deviation and the accuracy parameters, bias and relative recovery.

With a bias of 21%, the biosensor is considered accurate when determining the concentration of TNFα when this cytokine is diluted in a solution of 0.9% NaCl. The small divergence that does exist can be justified by the fact that the calibration was made using DI water as the medium. If the calibration curve had been obtained using the same solution as the testing samples, the measured R_{et} would take into account the dissolved salt and the resulting interpolation would more accurately represent the relation between TNFα concentration and normalized R_{et}.

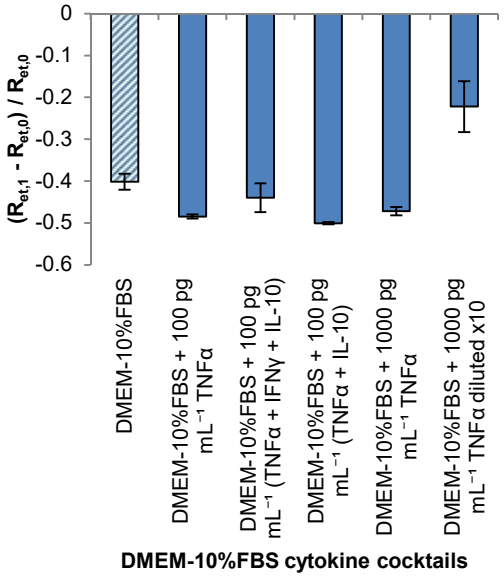

Figure 10: Normalized Ret and standard deviation for each DMEM-10%FBS cytokine cocktail incubated, including the blank, in striped blue.

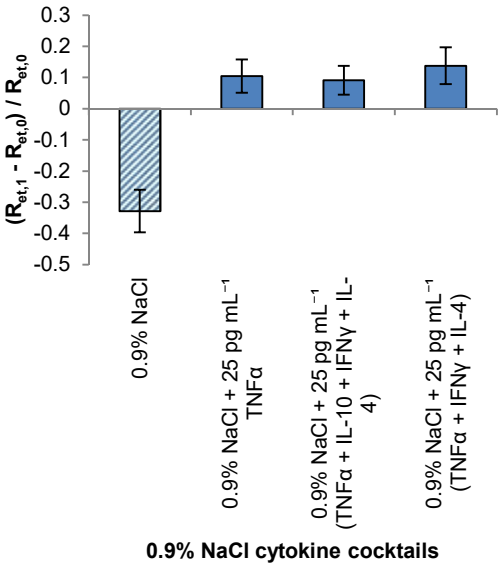

Figure 11: Normalized Ret and standard deviation for each 0.9% NaCl cytokine cocktail incubated, including the blank, in striped blue.

As for the cocktails with multiple cytokines, these present very minor relative recoveries, with -4.4% for the cocktail containing IL-10 and 11% for the cocktail without IL-10, meaning the sensor yield accurate results without interference by other cytokines in solution. Although IL-10 is, as discussed, a possible cross-reactant for this sensor, as it caused some interference in the measurements, it didn't seem to affect the biosensor's performance in this context. The similarity of the results between the cocktails might mean that TNFα always binds to the antibodies, even when competing with IL-10. Another possibility is that both TNFα and IL-10 are equally detected by the biosensor, as they are present in the cocktail in the same concentration. To test this, different cocktails with the same concentration of TNFα and different amounts of IL-10 should be analysed, as well as re-running the selectivity assays with the cytokines diluted in 0.9% NaCl to discern any effect of the salt on the cytokine IL-10.

3.5 Cross-validation with ELISA

For the ELISA cross-validation a calibration curve was build according to the instructions on the kit, which means the standards were diluted in DI water like those used for the biosensor calibration. The absorbance of a blank measurement was subtracted from the standards and the calibration curve obtained is shown in Figure 12 and the linear regression is Equation 2. In Table 3 are the interpolated concentrations, the standard deviation and the accuracy parameters, bias and relative recovery.

$$\text{Absorbance} = (1.07 \pm 0.06) \times 10^{-3} \times [\text{TNF}\alpha](\text{pg mL}^{-1}) + +(0 \pm 1) \times 10^{-2} \quad (2)$$

The concentrations interpolated for each cocktail are considerably higher than the expected 25 pg mL^{-1}. The solution with just TNFα has a positive bias of 97%, which suggests that the NaCl interferes with the efficiency of the assay, possibly with the antibodies capability of binding cytokines, binding more than they should, perhaps promoted by the ions in the solution. As with the cross-reactivity tests, this inaccuracy could be lessened by having the calibration curve be built with standards diluted in 0.9% NaCl, instead of DI water, to account for the effect of the dissolved salt.

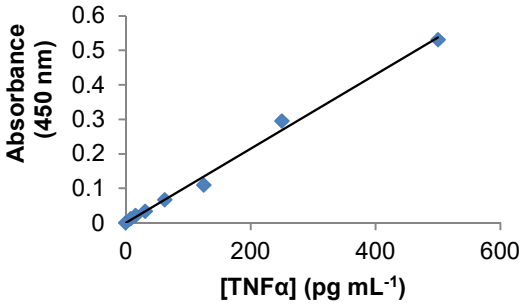

Figure 12: Calibration curve for the ELISA and linear regression.

Table 2: TNFα concentrations for each 0.9% NaCl cytokine cocktail, interpolated from the calibration curve in Equation 1, standard deviation and accuracy parameters: bias and relative recovery.

Cocktails	Average ΔR_{et}_TNFα	Interpolated [TNFα] (pg mL^{-1})	Standard Deviation (pg mL^{-1})	Accuracy	
				Bias	Relative Recovery
0.9% NaCl + 25 pg mL^{-1} TNFα (- blank)	0.432	$(3.0 \pm 0.9) \times 10^{1}$	3.77	21%	
0.9% NaCl + 25 pg mL^{-1} TNFα + 25 pg mL^{-1} IFN-γ + 25 pg mL^{-1} IL-4 + 25 pg mL^{-1} IL-10 (- blank)	0.419	$(2.9 \pm 0.9) \times 10^{1}$	3.62		-4.4%
0.9% NaCl + 25 pg mL^{-1} TNFα + 25 pg mL^{-1} IFN-γ + 25 pg mL^{-1} IL-4 (- blank)	0.466	$(3.3 \pm 1) \times 10^{1}$	4.14		11%

Table 3: TNFα concentrations for each 0.9% NaCl cytokine cocktail, interpolated from the calibration curve in Equation 2, from ELISA. Also featured are the standard deviation and accuracy parameters: bias and relative recovery.

Cocktails	Average Absorbance (450 nm)	Interpolated [TNFα] (pg mL^{-1})	Standard Deviation (pg mL^{-1})	Accuracy	
				Bias	Relative Recovery
0.9% NaCl + 25 pg mL^{-1} TNFα (- blank)	0.053	(5±2)x10^{1}	11.2	97%	
0.9% NaCl + 25 pg mL^{-1} TNFα + 25 pg mL^{-1} IFN-γ + 25 pg mL^{-1} IL-4 + 25 pg mL^{-1} IL-10 (- blank)	0.062	(6±2)x10^{1}	11.1		32%
0.9% NaCl + 25 pg mL^{-1} TNFα + 25 pg mL^{-1} IFN-γ + 25 pg mL^{-1} IL-4 (- blank)	0.056	(5±2)x10^{1}	11.1		10%

The relative recovery measured for the cytokine cocktails that contained more cytokines than TNFα is low, with values of 33% and 10%. This suggests that the ELISA, while suffering interferences from the NaCl, is still quite selective for TNFα in cocktails with different cytokines.

3.6 INL sensors

The functionalization protocol followed for the last calibration estimated for the INL electrodes was cleaning with Acetone/IPA/Milli-Q water, an overnight incubation with 10 mg mL^{-1} of Sulfo-LC-SPDP, an incubation of 120 minutes with 0.25 mg mL^{-1} antibody and 60 minutes with 1% BSA, followed by an overnight incubation in PB at 4º C. On the next day, the various concentrations of TNFα were incubated successively for 1 hour each, after a first PB incubation for 60 minutes. The concentrations used were 1, 2.5, 5, 10 and 25 pg mL^{-1} of TNFα. The graph in Figure 13 correlates the concentration to the normalized R_{et}, with $R_{et,1}$ as the R_{et} measured after each TNFα concentration incubated and $R_{et,0}$ defined as the R_{et} after the 60 minutes PB incubation.

The linear range on this estimation is a well-defined line, with positive normalized R_{et} values even for the lowest concentration levels. This suggests that the biosensors made with INL chips may have a lower LOD than the DropSens ones.

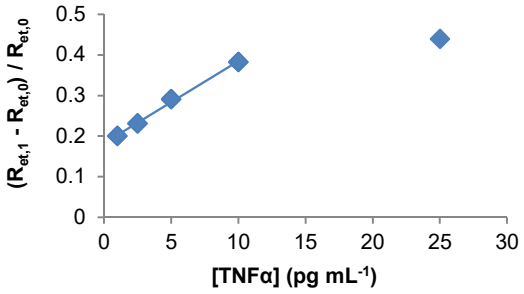

Figure 13: Variation of normalized Ret with TNFα concentration, for the electrode functionalized on the INL chip. A linear regression denotes the linear range and represents the calibration curve.

4 Conclusions

The biosensor is capable of detecting and quantifying TNFα, with an LOD of 2.6 pg mL^{-1}, lower than the ELISA's, as well as significantly less sample volume and incubation time. Of the three different control cytokines tested, the biosensor showed selectivity against IL-4 and IFN-γ and a small interference for IL-10, and performed with only a small bias in accuracy when tested on cytokine cocktails in 0.9% NaCl, despite the interferences caused by the salt.

With calibrations made with a single concentration level on each electrode and on the same media as the testing samples, more accuracy in future assays is to be expected. Resuming future work on the chips fabricated at INL should lead to higher precision and accuracy in results.

In the future, a more precise and accurate biosensor should be obtained to be used to test minimally invasive body fluids for the presence of cytokines. From that point on, a non-invasive, accurate and fast method for the diagnosis of neuroinflammation as a point-of-care device should soon be a reality.

References

1. Barres, B. A. The Mystery and Magic of Glia: A Perspective on Their Roles in Health and Disease. *Neuron* **60,** 430–440 (2008).
2. Ransohoff, R. M. A polarizing question: do M1 and M2 microglia exist? *Nat. Neurosci.* **19,** 987–91 (2016).
3. Ajami, B., Bennett, J. L., Krieger, C., Tetzlaff, W. & Rossi, F. M. V. Local self-renewal can sustain CNS microglia maintenance and function throughout adult life. *Nat. Neurosci.* **10,** 1538–43 (2007).
4. Pont-Lezica, L. *et al.* Microglia shape corpus callosum axon tract fasciculation: Functional impact of prenatal inflammation. *Eur. J. Neurosci.* **39,** 1551–1557 (2014).

5. Fariñas, I., Cano-Jaimez, M., Bellmunt, E. & Soriano, M. Regulation of neurogenesis by neurotrophins in developing spinal sensory ganglia. *Brain Res. Bull.* **57,** 809–816 (2002).

6. Ueno, M. *et al.* Layer V cortical neurons require microglial support for survival during postnatal development. *Nat. Neurosci.* **16,** 543–551 (2013).

7. Davalos, D. *et al.* ATP mediates rapid microglial response to local brain injury in vivo. *Nat. Neurosci.* **8,** 752–8 (2005).

8. Voyvodic, J. T. Cell death in cortical development: How much? Why? So what. *Neuron* **16,** 693–696 (1996).

9. Shrikant, P. & Benveniste, E. N. The central nervous system as an immunocompetent organ: role of glial cells in antigen presentation. *J. Immunol.* **157,** 1819–22 (1996).

10. Lettau, M., Schmidt, H., Kabelitz, D. & Janssen, O. Secretory lysosomes and their cargo in T and NK cells. *Immunol. Lett.* **108,** 10–19 (2007).

11. Rock, R. B. *et al.* Role of Microglia in Central Nervous System Infections Role. *Clin. Microbiol. Rev.* **17,** 942–64 (2004).

12. Wood, P. L. in *Neuroinflammation: Mechanisms and management* 3–27 (2003).

13. Chhor, V. *et al.* Characterization of phenotype markers and neuronotoxic potential of polarised primary microglia In vitro. *Brain. Behav. Immun.* **32,** 70–85 (2013).

14. Colton, C. a. Heterogeneity of microglial activation in the innate immune response in the brain. *J. Neuroimmune Pharmacol.* **4,** 399–418 (2009).

15. Perry, V. H. & Holmes, C. Microglial priming in neurodegenerative disease. *Nat. Rev. Neurol.* **10,** 217–24 (2014).

16. Liao, B., Zhao, W., Beers, D. R., Henkel, J. S. & Appel, S. H. Transformation from a neuroprotective to a neurotoxic microglial phenotype in a mouse model of ALS. *Exp. Neurol.* **237,** 147–152 (2012).

17. Hickman, S. E., Allison, E. K. & El Khoury, J. Microglial dysfunction and defective beta-amyloid clearance pathways in aging Alzheimer's disease mice. *J. Neurosci.* **28,** 8354–60 (2008).

18. Imamura, K. *et al.* Distribution of major histocompatibility complex class II-positive microglia and cytokine profile of Parkinson's disease brains. *Acta Neuropathol.* **106,** 518–526 (2003).

19. Cartier, N., Lewis, C. A., Zhang, R. & Rossi, F. M. V. The role of microglia in human disease: Therapeutic tool or target? *Acta Neuropathologica* **128,** 363–380 (2014).

20. Nakamura, Y. Regulating factors for microglial activation. *Biol. Pharm. Bull.* **25,** 945–953 (2000).

21. Aloisi, F., De Simone, R., Columba-Cabezas, S. & Levi, G. Opposite effects of interferon-γ and prostaglandin E2 on tumor necrosis factor and interleukin-10 production in microglia: A regulatory loop controlling microglia pro- and anti-inflammatory activities. *J. Neurosci. Res.* **56,** 571–580 (1999).

22. Makita, N., Hizukuri, Y., Yamashiro, K., Murakawa, M. & Hayashi, Y. IL-10 enhances the phenotype of M2 macrophages induced by IL-4 and confers the ability to increase eosinophil migration. *Int. Immunol.* **27,** 131–141 (2015).

23. Bienvenu, J., Monneret, G., Fabien, N. & Revillard, J. P. The Clinical Usefulness of the Measurement of Cytokines. *Clin. Chem. Lab. Med.* **38,** 267–285 (2000).

24. Hagan, S. *et al.* Tear fluid biomarkers in ocular and systemic disease: potential use for predictive, preventive and personalised medicine. *EPMA J.* **7,** 15 (2016).

25. eBioscience. Human TNF alpha ELISA Ready-SET-Go!®. Available at: http://www.ebioscience.com/human-tnf-alpha-ready-set-go-elisa.htm. (Accessed: 4th December 2016)